Available online at www.sciencedirect.com
SCIENCE DIRECT®
Journal of Sound and Vibration 262 (2003) 347–364
JOURNAL OF SOUND AND VIBRATION
www.elsevier.com/locate/jsvi

# Noise attenuation by a hard wedge-shaped barrier

D. Ouis

*School of Technology and Society, Malmö University, Gaddan 8, SE-205 06 Malmö, Sweden*

Received 3 September 2001; accepted 24 April 2002

**Abstract**

This paper is concerned with the problem of sound screening by a wedge-like barrier. The sound source is assumed to be point like, and the receiver is located in the shadow of the source sound field, so that according to geometrical optics only the field diffracted by the edge of the barrier is considered. First, for the hard wedge in space, three models are used for calculating the amplitude of the edge-diffracted field. These are the uniform theory of diffraction (UTD), the Hadden–Pierce model, both in the frequency domain, and the Biot–Tolstoy theory of diffraction which is a time domain formulation. It is first shown that even at relatively low frequencies, the frequency domain models perform quite satisfactorily as compared to the exact time domain theory. Hence, and due to its relative simplicity the UTD is proposed as an accurate calculation scheme for solving problems with edge diffraction by hard wedges. It is also proved from theoretical calculations that the amplitude of the edge-diffracted field increases for an increasing angle of the wedge, and consequently the hard half-plane gives the lowest field amplitude in the shadow zone. Some applications are then considered for evaluating the performance of a barrier on a flat ground, either completely hard or with mixed homogeneous boundary conditions. An improvement of the scheme for calculating the sound field in the all-hard case is achieved through considering the multiple diffraction, in this case only to the second order, between the top of the wedge barrier and its base. The results show that for usually occurring situations, increasing the angle of the hard wedge barrier affects negatively its efficiency through diminishing its insertion loss. These conclusions are also supported by the results of some experimental measurements conducted at a scale-model level.


## 1. Introduction

Noise emitted by rolling vehicles constitutes a serious problem for people dwelling nearby roads. Barriers are thus often used in residential areas for reducing this noise emanating from

*E-mail address:* djamel.ouis@ts.mah.se (D. Ouis).

0022-460X/03/$ - see front matter © 2002 Elsevier Science Ltd. All rights reserved.
doi:10.1016/S0022-460X(02)01134-3

traffic. However, researchers are often in need of theoretical prediction schemes enabling them to foresee the performance of newly designed noise-reducing devices before installing them or running full-scale tests on their prototypes. Theoretical predictions in the case of noise barriers are usually based on either numerical techniques like the boundary and the finite element methods (BEM and FEM), or on analytical models. In this latter case, a simplified calculation scheme would be the combination of a model for describing the reflection of sound waves on the ground and a model that takes into consideration the phenomenon of wave diffraction by straight-edged objects. For a general overview of the different theories and techniques that have been developed for handling the problem of wave diffraction around semi-infinite objects reference is made to the Bowman et al. work [1] and to the classical works of Macdonald [2], Bromwich [3], Whipple [4], and Carslaw [5].

During the past few decades there has been an intensive research activity in the field of noise abatement by barriers, and as a consequence several accurate models have been developed both for acoustical wave reflections at a flat impedance ground, and for wave propagation around semi-infinite geometries. Already from the late 1950s or so, several authors contributed to the development of numerous solution strategies to the problem of sound diffraction by simple screens and with particular applications to traffic noise barriers. Some of the more recently published results on the problem of the simple hard wedge in space include those of Oberhettinger [6,7], Garnir who presented the expression for the Green functions for the wedge with ideal hard or ideal soft faces [8], Friedlander [9], Maliuzhinets [10], Kusnetzov [11], Osipov and Norris [12], Thuzilin [13], Biot and Tolstoy [14], Tolstoy [15,16], and Buckingham and Tolstoy [17]. Keller and Blank [18], Lee et al. [19], and Büyüdkura [20], processed also various improvements to the then popular geometrical theory of diffraction (GTD), while Kawai expressed the field diffracted by a pillar with many sides through a consideration of the mutual interaction between the waves diffracted by the edges of the pillar [21]. A similar approach was also taken by Elsherbeni and Hamid [22] and Robertson [23] to treat the case of a wide truncated wedge. The work of Kouyoumjian and Pathak is also worth mentioning in this context as their solution to the wedge problem is another more elaborated version of the GTD remedying the main failure of continuity of the total field at the geometrical transition regions [24]. Ambaud and Bergassoli [25], Pierce [26] (who treated the case of a truncated wedge by adding higher terms accounting for the double edge diffraction), and Hadden and Pierce [27,28] gave more tractable approximations to classical solutions of the problem with useful expressions of the sound pressure field around a hard wedge for specific positions of the sound source and the receiver. Mechel treated the problem of wedge scattering by means of modal analysis and showed how sound sources can be introduced in the wedge apex, and how to treat these field singularities [29].

The problem of the wedge has also attracted the interest of researchers in electromagnetism with applications to the design of antennas and reflectors, and to the prediction of wave scattering by perfectly conducting metallic or dielectric wedges. Solutions are given for different kinds of wave incidence, and that in comparison to the size of the scattering object, the range of wavelengths in the electromagnetic case may be several orders of magnitude smaller than that of sound waves, these solutions have often been successfully implemented to the acoustical case [30–46]. The acoustical counterpart of the dielectric case in electromagnetism is that of a wedge with surfaces of general impedance boundary conditions, a problem also treated by some authors with various different methods [10, 47–50].

Some of the other more specific problems involving the wedge geometry include the cases of a finite wedge where the diffracted field is evaluated through a line integral over the illuminated part of the wedge. The knowledge of the diffraction coefficients for the ideal boundary cases permitted the development of the notion of equivalent currents, which are basically fictitious currents used to account for the field diffracted by the edge of impedance structures [51–53]. A closely related method uses the notion of incremental diffraction length coefficients [54,55]. Another extension of the GTD to imperfect wedges includes also numerical techniques [45,56] as well as heuristic methods based on other exact methods for the determination of GTD coefficients [57–58].

Other various applications of wedge-shaped scattering wedges make reference to Mechel's work where a study of the problem of sound propagation in wedge-shaped ducts permits the determination of the mode configuration for this particular type of ducts [59,60]. Other related works, but more relevant to the propagation of sound in a submarine environment with a hilly bottom, are due to Buckingham [61] (with either perfectly hard, pressure release or mixed boundary conditions on the faces of the wedge), Graves et al. [62], Felsen and Kuperman [63] and Arnold and Felsen [64] mostly with the method of expressing the field as the sum of normal modes in a similar manner as that used earlier by Biot and Tolstoy [14]. In conjunction to this, it is worthwhile mentioning that Kinney et al. extended the solution to include the case of a perfectly soft wedge, with simple sign changes introduced on some of the terms expressing the diffracted field [65].

## 2. Theory: diffraction of a spherical wave by a hard wedge

In this section, comparison is made between the performance of three different models used for the calculation of the edge diffraction of a spherical wave by a hard wedge. Fig. 1 illustrates the geometry of the wedge with the different parameters needed later for calculations. Throughout the whole paper the time dependence of the field variables is omitted and is taken in accordance with the theory in the original works, that is $e^{j\omega t}$, except for the next section where it is taken as $e^{-j\omega t}$.

### 2.1. The UTD

From a geometrical point of view, if the incident field is $u_i = A(R)e^{-ikr(R)}$, $kr(R)$ being the phase along the ray and $k$ the wavenumber, the diffracted field $u_d$ a distance $r$ from the diffraction point

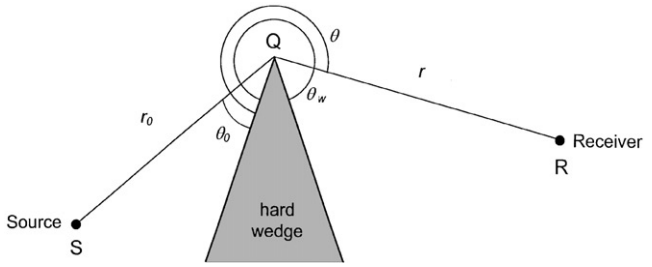


Fig. 1. Geometry of the problem of diffraction of a spherical acoustical wave by a hard wedge.

is given by [24]

$$u_d(R) = u_i(Q)A(r', r)D_h e^{-ikr}, \tag{1}$$

where $u_i(Q)$ is the incident field at the point of diffraction $Q$ on the edge, $A(r', r)$ the coefficient depending on the characteristics of the source of the primary rays, $r'$ being the distance from the source to $Q$ in case the source is either cylindrical or spherical. The diffraction point $Q$ is the point on the diffracting edge making minimum the path from the source to the receiver via the diffracting edge. The coefficient $D_h$ depends on the angles of the incident and the diffracted rays and on the diffracting screen, and $h$ denotes the hard type of boundary on the screen. For spherical wave incidence the expressions of the coefficients $A$ and $D_h$ are, respectively, given by

$$D_h = \frac{-e^{-i\pi/4}}{2n\sqrt{2\pi k}\sin\zeta}\left\{\cot\left(\frac{\pi+(\theta-\theta_0)}{2n}\right)F[kLa^+(\theta-\theta_0)] + \cot\left(\frac{\pi-(\theta-\theta_0)}{2n}\right)F[kLa^-(\theta-\theta_0)]\right.$$
$$\left. + \cot\left(\frac{\pi+(\theta+\theta_0)}{2n}\right)F[kLa^+(\theta+\theta_0)] + \cot\left(\frac{\pi-(\theta+\theta_0)}{2n}\right)F[kLa^-(\theta+\theta_0)]\right\} \tag{2}$$

and

$$A(r', r) = \sqrt{\frac{r'}{r(r'+r)}}, \tag{3}$$

$L$ being a distance parameter given by

$$L = \frac{rr'}{r+r'}\sin^2\zeta \tag{4}$$

and $F(X)$, sometimes referred to as the transition function is a form of Fresnel integral

$$F(X) = 2i\sqrt{X}e^{iX}\int_{\sqrt{X}}^{\infty} e^{-i\tau^2}\,d\tau. \tag{5}$$

The argument $a^{\pm}$ is expressed by

$$a^{\pm}(\alpha) = 2\cos^2\left(\frac{2n\pi N^{\pm}-\alpha}{2}\right), \tag{6}$$

in which $N^{\pm}$ is an integer which most nearly satisfies the equality $2\pi nN^{\pm}-\alpha = \pm\pi$. The parameter $n$ is a measure of the wedge angle, and is given by $n = \theta w/\pi$ taking the value of 2 for a half-plane. The angle made by the incident ray with the normal to the edge at the point of diffraction is $\zeta$ (according to the UTD, this angle is also equal to that made by the diffracted ray and the normal). In what follows only the case of normal incidence is considered, that is $\zeta = 90^\circ$. In this case, the diffraction point is found simply as the intersection point between the edge of the wedge and the plane normal to it and containing the source and receiver points.

The expression of the diffracted field as given in Eq. (1) ensures that the total field is continuous throughout all space because the discontinuities in the geometrical optics field components are exactly compensated by those in the diffracted field at traversing the geometrical incidence and reflection boundaries.

### 2.2. The Biot–Tolstoy (B–T) theory of diffraction

This theory is exact and in the time domain. For a Dirac pulse from a point source $S$

$$u = \frac{\rho A}{4\pi R}\,\delta\left(t - \frac{d}{c}\right), \tag{7}$$

where $d$ is the distance range from the sound source and, the amplitude of the edge-diffracted wave is [14, 66]

$$u_d(t) = \frac{-A\rho c}{4\pi\theta_W}\,\{\beta\}\,\frac{\exp(-vy)}{rr_0\sinh(y)}. \tag{8}$$

Then, the B–T theory predicts, as mentioned earlier, the eventual existence of a direct, one or two reflected pulses depending on the wedge angle and the positions of $S$ and $P$, and a diffracted wave due to the tip of the wedge. This diffracted wave appears at a time $\tau_0$ after the source has emitted its spherically divergent pulse

$$\tau_0 = [(r + r_0)^2 + z^2]^{1/2}/c, \tag{9}$$

where $\tau_0$ is called the least time over the wedge, $r_0$ and $r$ are the normal distances to the wedge of, respectively, the source and the receiver, and $z$ the lateral distance between them. In Eq. (8) the expression of $y$ is given by

$$y = \operatorname{arccosh}\frac{c^2t^2 - (r^2 + r_0^2 + z^2)}{2rr_0}, \tag{10}$$

and $\{\beta\}$ is the sum of four terms with different addition signs in the argument of the trigonometric functions in

$$\{\beta\} = \frac{\sin[v(\pi \pm \theta \pm \theta_0)]}{1 - 2\exp(-vy)\cos[v(\pi \pm \theta \pm \theta_0)] + \exp(-2vy)}, \tag{11}$$

with $c$ the speed of propagation of sound. The wedge index $v$ is in this case defined by $v = \pi/\theta w = 1/n$. The exact frequency form of Eq. (4) is not available in closed form, and therefore a numerical Fourier transform is used to evaluate it.

### 2.3. The Hadden–Pierce (H–P) model

The Green function solution for the diffraction of a spherical wave by a hard wedge is inspired by classical theory [8]. Approximations are necessary as a result of numerical difficulties faced in attempting to give closed-form solutions. These have been presented by Hadden and Pierce [27,28] for the cases where the receiver is situated in the far-field or at the geometrical shadow boundaries. Related work has reported agreement with carefully mounted experiments [25], as well as that the model has been applied to diffraction of acoustic impulses [67].

The solution to the Helmholtz equation satisfying the hard boundary conditions, $\partial u/\partial n = 0$, on the sides of the hard wedge $\theta = 0$ and $\theta_w$ (see Fig. 1) may be expressed as

$$u = \sum_{i=1}^{4}[u(\xi_i)\mathrm{H}(\pi - \xi_i) + u_d(\xi_i)], \tag{12}$$

where

$$\xi_1 = |\theta_0 - \theta|, \quad \xi_2 = 2\theta_W - \xi_1, \quad \xi_4 = \theta + \theta_0, \quad \xi_3 = 2\theta_W - \xi_4 \tag{13a-d}$$

and $H(\alpha)$ is the Heaviside unit step function.

The first three terms of the field are found from pure geometrical considerations, that is for $i = 1$, 3 and 4, $u(\xi_i)H(\pi - \xi_i)$ represent, respectively, the direct and the reflected waves from the sides $\theta = 0$ and $\theta_w$ of the wedge. $\xi_2$ being always greater than $\pi$, the term $u(\xi_2)H(\pi - \xi_2)$ is always zero and is written only for the tractability of the expression for the field. The $u(\xi_i)$ are supposed to be of the form $e^{ikR_i}/R_i$ with

$$R_i = [r^2 + r_0^2 + z^2 - 2rr_0 \cos \xi_i]^{1/2}. \tag{14}$$

The sum on the left-hand side of the expression for the total field (Eq. (12)) ($\sum_{i=1}^{4} u_d(\xi_i)$) may be interpreted as a diffracted wave. For each $\xi_i$, $u_d$ is expressed as an integral of the form

$$u_d(\xi_i) = -\frac{1}{\pi}\int_0^{\infty} u(\pi + iw)Q(w, v, \xi_i)\, dw, \tag{15}$$

where

$$Q(w, v, \xi_i) = \frac{(v/2)\sin[v(\pi - \xi_i)]}{\cosh(vw) - \cos[v(\pi - \xi_i)]}, \tag{16}$$

$v = \pi/\theta w$ being the wedge index seen earlier, and $u(\pi + iw)$ is the previous $e^{ikR}/R$, but now with $\xi$ in Eq. (14) replaced by $(\pi + iw)$.

Because of the oscillatory character of the integral in Eq. (15), its direct numerical evaluation presents some difficulties, but some useful approximations for the most practical cases have been presented. Hence, a new form for the integral is presented with a new parameter $A$

$$A(\xi_i) = (v/2)(-\theta_w - \pi + \xi_i) + \pi H(\pi - \xi_i), \tag{17}$$

and with this in mind the new expression of $u_d$ is reformulated as

$$u_d(\xi_i) = (-1/\pi)A(\xi_i)(e^{ikL}/L)F_v(|A|, \alpha, \varepsilon) \tag{18}$$

in which

$$F_v(|A|, \alpha, \varepsilon) = \int_0^1 I(q)\, dq, \tag{19}$$

$$\alpha = krr_0/L, \quad \varepsilon = rr_0/L^2, \quad L = [(r + r_0)^2 + z^2]^{1/2}, \tag{20}$$

$$I(q) = (L/R)e^{ik(R-L)}. \tag{21}$$

The quantity $L$ is the least time path, i.e., the shortest two segment distance from the point source to the field point via the edge, and is simply equal to the product of the least time $\tau_0$ in Eq. (9) and the speed of sound $c$.

Approximations of $u_d$ for different values of $A$, $\alpha$ and $\varepsilon$ are presented next. For the case at hand, the following results are obtained. When both the source and the receiver are far from the edge of

the wedge, $\alpha = krr_0/L \gg 1$ and $|A|$ is arbitrary, one has [27]

$$F_v(|A|, \alpha, \varepsilon) \cong \frac{\pi}{\sqrt{2}} \frac{\sin|A|}{|A|} \frac{e^{i\pi/4}}{[1 + (2\varepsilon + 1/2)\cos^2|A|/v^2]^{1/2}} A_D(P), \tag{22}$$

with

$$A_D(p) = \frac{P}{\sqrt{\pi}} \int_0^{\infty} \frac{e^{-u^2}}{(\pi/2)P^2 + iu^2} du = f(P) - ig(P) \tag{23}$$

and

$$P = \left(\frac{4\alpha}{\pi}\right)^{1/2} \frac{\cos|A|}{[v^2 + (2\varepsilon + 1/2)\cos^2|A|]^{1/2}}. \tag{24}$$

### 2.4. Numerical comparison between the three models

The results of some calculations on the three models presented are illustrated in Fig. 2. The amplitude of the edge-diffracted wave was normalized to the free-field spherical wave at a source–receiver distance equal to $r + r_0$. The distances $r_0$ and $r$ were chosen, respectively, 2 and 4 m, and the wavelength of the signal was taken for values ranging from $\lambda = r_0/100$ to $10r_0$. The important observation from these last results is that even at the lowest frequency considered, the two approximate models have a very satisfactory performance as compared to the exact theory, the frequency form of this latter being evaluated from Eq. (8) through a numerical Fourier transform. The increase of the field amplitude of the edge-diffracted field is more accentuated at wedge angles greater than 90°. Similarly, for the special case of the half-plane, and for fixed positions of the source and the receiver, the amplitude of the edge-diffracted field decreases by about 2.5 dB for each doubling of the frequency. From an engineering point of view, and due to the relative ease of

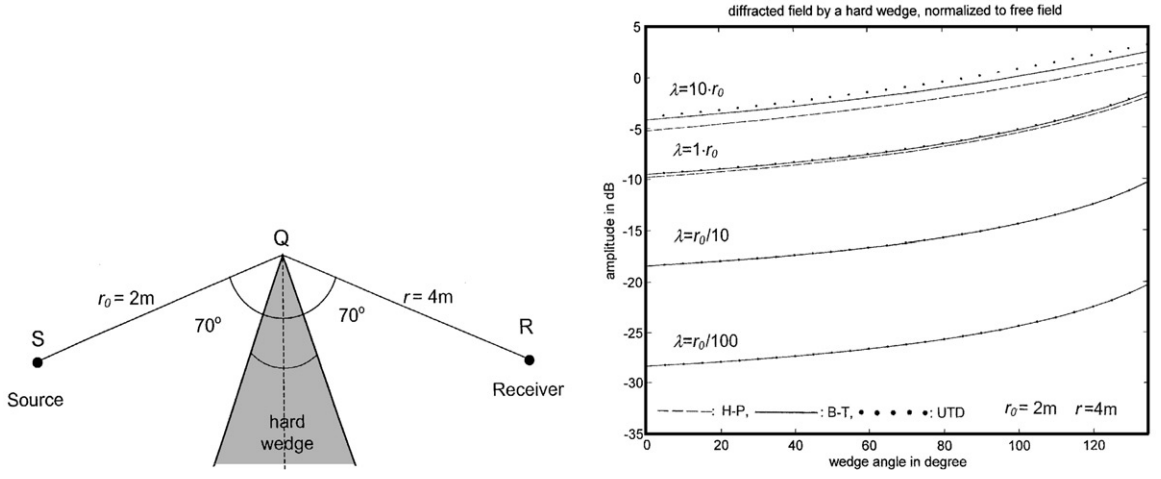


Fig. 2. Diffraction of a spherical wave by a hard wedge. Left: geometry; Right: theoretical comparison between three models.

its implementation in calculation procedures, the UTD is an attractive alternative tool for calculations on problems with hard wedges.

## 3. Reflection of a spherical wave at an impedance boundary

Usually, the total field above a reflecting boundary is expressed as the sum of three components, which are the direct field source–receiver, the field from the image source through the boundary as if it were perfectly hard, and a correction term which takes into account the impedance of the boundary.

### 3.1. Case of a boundary with a homogeneous impedance: Thomasson's model

According to this model, the total field at the receiver is made of three contributions: a direct wave with the distance range $R_1$, a reflected wave with $R_2$ as if the ground were perfectly hard, and a correction term taking into account the complex and finite impedance of the ground [68]. Let $v$ be the specific point admittance of the boundary, i.e., $v = \rho c/Z$, with $\rho$ the density of air.

Then

$$u_{tot} = \frac{e^{ikR_1}}{4\pi R_1} + \frac{e^{ikR_2}}{4\pi R_2} - \Psi_R. \tag{25}$$

The details for calculating $\Psi_R$ are as follows:

$$\Psi_R = \begin{cases} \Psi_{SD} + \Psi_B & \mathrm{Re}(\gamma_0) > 1 \text{ and } \mathrm{Im}(v) < 0, \\ \Psi_{SD} & \text{else}, \end{cases} \tag{26}$$

$$\Psi_{SD} = \frac{kv}{2\pi} e^{ikR_2} \int_0^\infty \frac{e^{-kR_2 t}}{\sqrt{W_1}} \mathrm{d}t, \tag{27}$$

$$W_1 = [\cos\alpha_0 + v]^2 + 2it[1 + v\cos\alpha_0] - t^2, \tag{28}$$

$$\mathrm{Re}(\sqrt{W_1}) \begin{cases} < 0 & \mathrm{Re}(\gamma_0) > 1,\ \mathrm{Im}(v) < 0,\ t > t_1, \\ > 0 & \text{else}, \end{cases} \tag{29}$$

$$t_1 = -\mathrm{Im}(v) \frac{\mathrm{Re}(v) + \cos\alpha_0}{1 + \cos\alpha_0\, \mathrm{Re}(v)}, \tag{30}$$

$$\Psi_B = \frac{1}{2} kv H_0^{(1)} \left[ k(x_S + x_R)\sqrt{1 - v^2} \right] e^{-ik(y_S + y_R)v}, \tag{31}$$

$$\gamma_0 = -v\cos\alpha_0 + \sqrt{1 - v^2}\sin\alpha_0, \quad \mathrm{Re}\left[\sqrt{1 - v^2}\right] > 0. \tag{32}$$

The term $\Psi_B$ as given in Eq. (26) has been termed as a "surface wave" by Thomasson who invites however some caution on the general use of this expression. This is because only in some cases, like the one of a "finite impedance" boundary that it may be possible to theoretically split the total field into two physical components, a "space wave" term and a "surface wave" term and that

in more general instances it may not be well justified to always associate physically a surface wave with the function $\Psi_B$.

### 3.2. Case of a boundary with an impedance discontinuity: deJong et al. model

To evaluate the insertion loss of a barrier on the ground, it is often necessary to have at hand a calculation scheme enabling one to evaluate the field due to a sound source in the presence of a flat boundary with an impedance discontinuity. For not too extreme geometrical situations, the simple, and reasonably efficient model presented by deJong et al. [69] states that assuming that the free-field source–receiver is $u_f$, the excess attenuation due to the introduction of the two-impedance boundary is given according to (the line of impedance discontinuity is assumed to be normal to the line joining the sound source to the receiver)

$$\frac{u}{u_f} = 1 + \frac{R_1}{R_2} Q_{1,2} e^{ik(R_2-R_1)} + \frac{R_1}{R_3}(Q_2 - Q_1)\frac{e^{-i\pi/4}}{\sqrt{\pi}}\left\{F\left[\sqrt{k(R_3 - R_1)}\right] \pm F\left[\sqrt{k(R_3 - R_2)}\right] e^{ik(R_2-R_1)}\right\}, \tag{33}$$

where $R_3$ is the two-segment distance source–receiver via the impedance discontinuity, and $Q_{1,2}$ are the spherical wave reflection coefficients for an infinite mono-impedance boundary, and which may be calculated according to Thomasson's exact theory or to the Chien and Soroka approximate theory [70]. The function $F(x)$ is the Fresnel integral defined by

$$F(x) = \int_x^\infty e^{iw^2}\, dw \tag{34}$$

and $Q_1(Q_2)$ with $+(-)$ are used in case the specular reflection point falls on the boundary nearer (farther) the sound source.

## 4. Numerical examples: a hard wedge-like barrier on the ground

With reference to Fig. 3, the total pressure field at the receiver may be considered as the sum of four components represented by the wave propagation paths source-top of barrier-receiver SHR, S′HR, SHR′ and S′HR′.

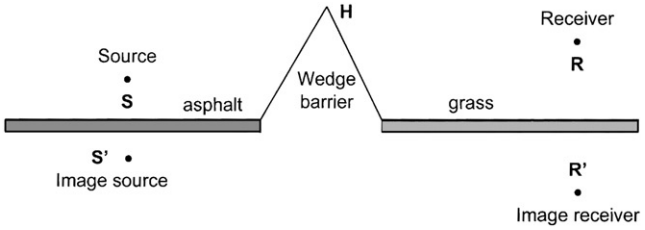


Fig. 3. Illustration of the wedge-shaped noise barrier on a flat ground.

This simplified modelling is used in almost all analytical approaches to this kind of problem and is valid as long as the frequency is not too low (usually down to a wavelength corresponding to a typical size of the problem). The primes on the letters refer to reflections on the ground and for instance, the path S′HR represents a wave radiated by the source, which then reflects on the ground (hence seems to originate at S′, the image of S through the ground), and proceeds afterwards to the receiver R after diffraction at the top H of the barrier. As an illustrative application of the theory exposed hitherto, calculations are made on a typical traffic noise situation. The efficiency of a noise barrier is evaluated in terms of its insertion loss, which is defined as the difference in dB of the sound levels at the receiver before, and after mounting the barrier on the ground.

### 4.1. Case of a perfectly hard ground

As the diffraction phenomenon considered here is applied to finite diffracting surfaces, a consideration of the interaction between the wedges at the top and at the base of the barrier is expected to improve the evaluation of its insertion loss. Hence the use of the notion of fictive sound sources on the diffracting edges. The calculation of the positions and strengths of these secondary sources follows the method as described by Medwin et al. [71]. The effect of the double diffraction is expected to be significant only for the contribution of the secondary sources lying at most proximity of the point of diffraction on the edge. Fig. 4 shows the curves of variation of the strength of the secondary sources as a function of their order number for the different double diffraction paths from the sound source to the receiver, the wedge angle being equal to 90°. With reference to Fig. 3, the co-ordinates of the various points were S(−5, 0.4 m), R(12, 1.8 m) and H(0, 3 m).

Fig. 5 (left) illustrates the variation of the strength of the secondary sources of order zero, that is the strongest fictive secondary source on the edge, as a function of the wedge angle. For the path along SBHB′R, the strength of the secondary sources is equal to that of the secondary sources along the path SBHB′R′ for the reason that the strength is determined from the diffracted field along the path SBH. Note the relatively slow variation of the sources strength along the paths SHB′R and S′HB′R. The corresponding amplitudes of the diffracted fields are plotted on the curves of the right-hand side of the same figure.

The calculations show a rapid decrease of the strength of the secondary sources for an increasing distance from the point of diffraction on the edge, and consequently only the 30 strongest secondary sources on either side of the diffraction point were taken into consideration in the calculations that follow.

Fig. 6 illustrates the variation with frequency of the insertion loss of a hard wedge-like barrier on a perfectly hard ground. The calculations were made through taking into account both the single diffraction at the top edge of the barrier, and through combining both the single and double diffraction.

### 4.2. Case of an absorbing ground with an impedance discontinuity

The efficiency of a simple wedge barrier is evaluated in this case when it is erected on a ground constituted of a combination of hard, asphalt-like boundary on the sound source side, and soft,

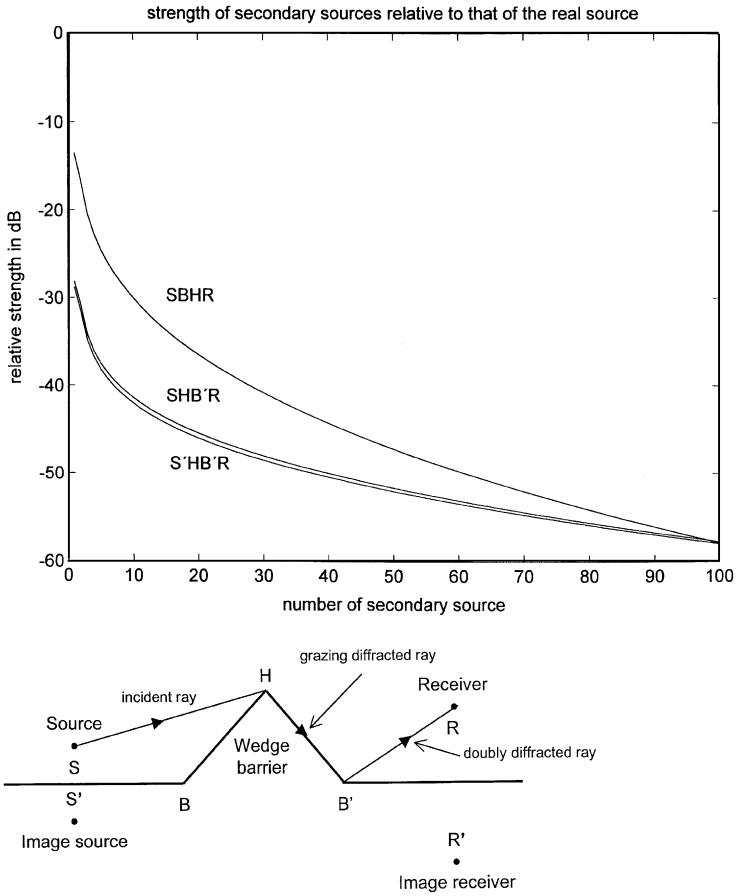


Fig. 4. Strength of the fictive secondary sources as a function of position on the edges for the different multiple diffraction paths. Wedge angle $w = 90^\circ$.

grass like on the receiver side. For calculating the overall sound levels, it is necessary to know the frequency variation of the boundary impedances over a wide frequency range. This latter was determined according to the Delany–Bazley one-parameter model provided that only the flow resistivity of the boundary material is known [72] (it should however been pointed out that the validity of this model is restricted to limited values of $f/\sigma$, $f$ being the frequency and $\sigma$ the flow resistivity). The flow resistivities of asphalt and grass were taken from the list of experimentally determined values as determined by Embleton et al. [73].

Fig. 7 illustrates the results for realistic situations, where are plotted the curves of the frequency variations of the sound pressure level in presence of barriers with different wedge angles. The curve for the case without barrier is plotted together with these curves. The calculations were performed at the standard one-third octave bands.

The curves for the variation of the insertion loss of a wedge barrier as a function of the top angle are illustrated in Fig. 8.

The results from these last two curves show the deterioration of the efficiency of the wedge barrier for an increasing value of its top angle. The sound pressure level variation with the

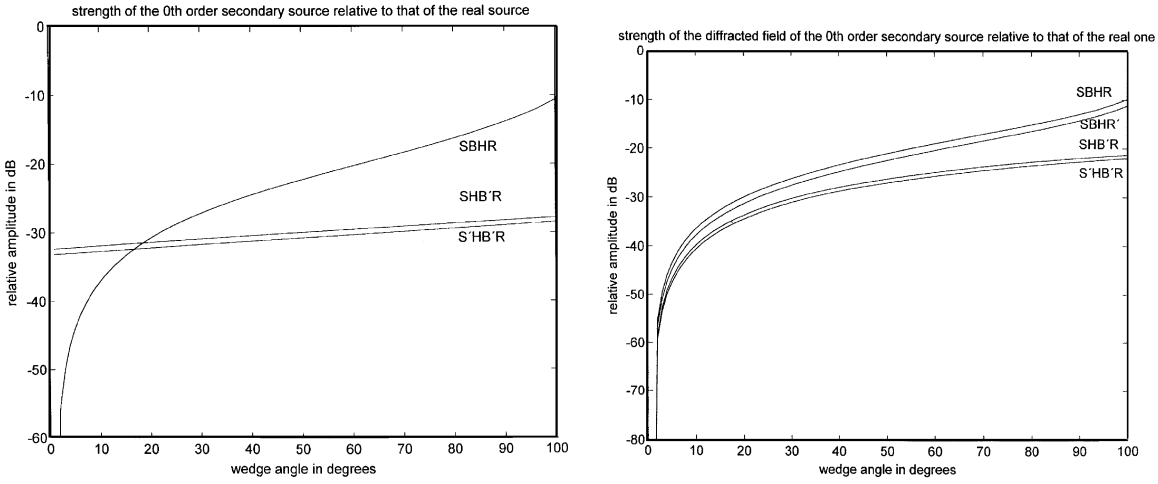


Fig. 5. Double diffraction at the top and bases of the barrier. Left: strength of the zeroth order secondary fictive source, normalized to that of the real sound source, as a function of the wedge angle. Right: strength of the corresponding double diffraction field as normalized to the direct diffracted field, path SHR.

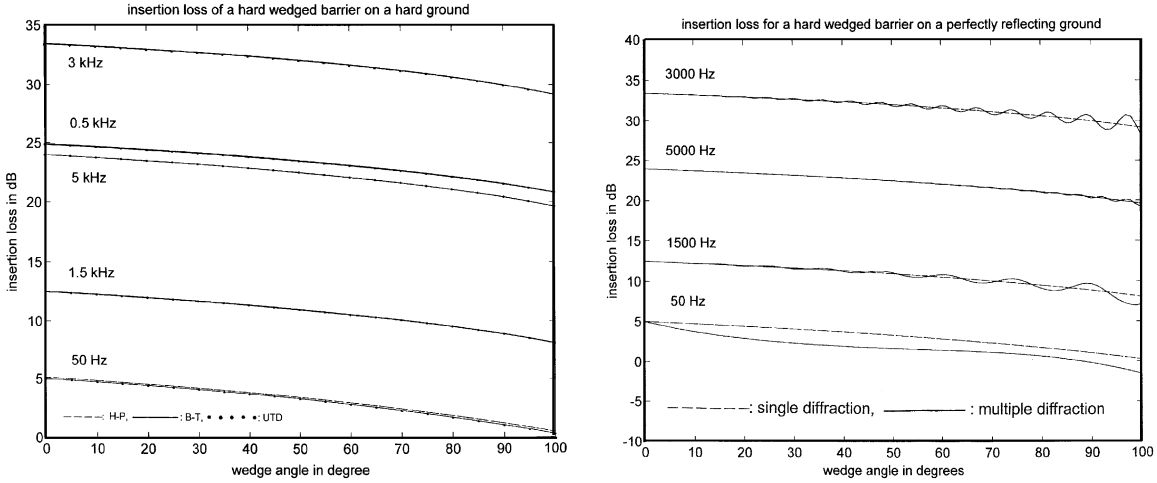


Fig. 6. Insertion loss of a wedge barrier on a hard ground for different frequencies. Left: single diffraction, all three calculation models. Right: single + double diffraction, B–T theory.

frequency is almost the same for the different wedge angles except that the curves are displaced towards higher dB values for barriers wider at the base.

## 5. Experiments at the scale-model level

As a last consideration of the problem of the wedge barrier, some experiments were conducted at the scale-model level to complement the theoretical study. It is to be mentioned that these experiments are of a rather qualitative character, and their results were not compared to their

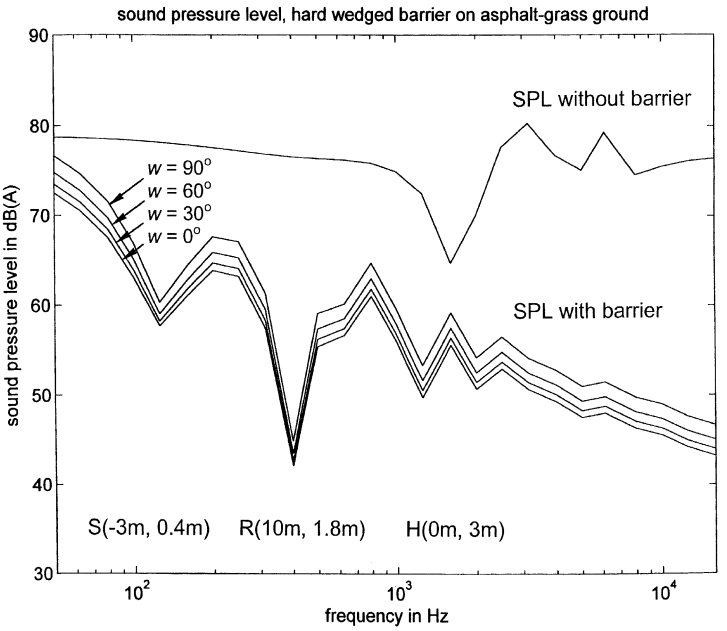


Fig. 7. Insertion loss of a hard wedge-like barrier on the ground. Variation with frequency for different wedge angles.

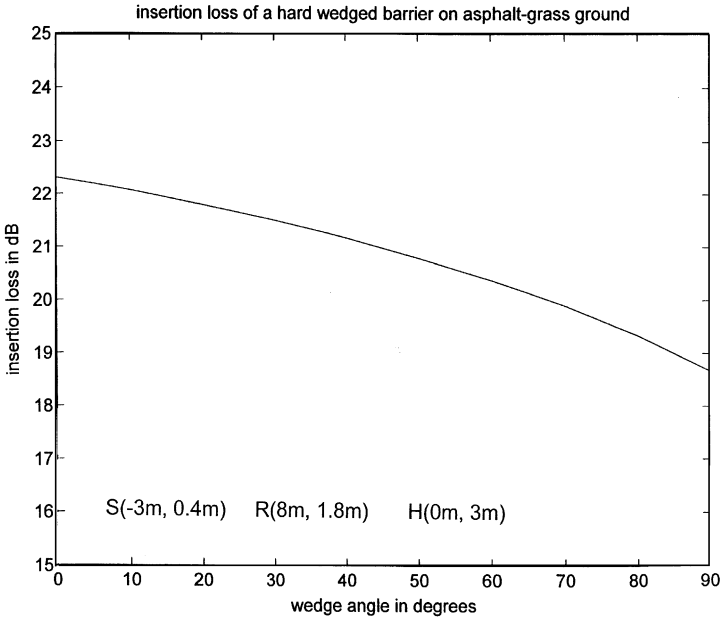


Fig. 8. Insertion loss of a hard wedge barrier on the ground. Variation with the wedge angle.

theoretical predictions. The geometry and sizes involved in the experimental set-up are shown in Fig. 9, and where the wedge barrier was realized by means of two 8 mm thick plywood planks fastened at the sharpened tops by screws.

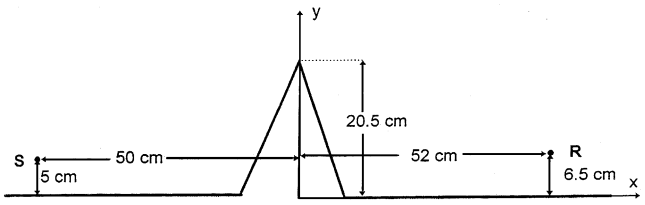


Fig. 9. Sound abatement by a wedge-shaped barrier: schematic illustration of the experimental set-up at the scalemodel size.

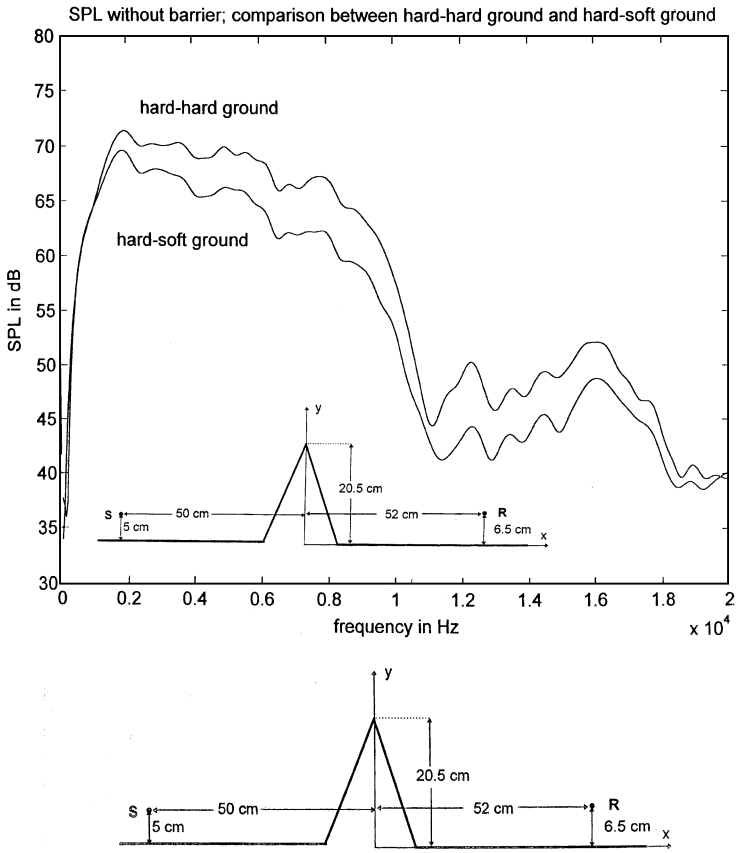


Fig. 10. Sound pressure level over a flat ground. ———: Hard ground, - - - - -: combination of hard–soft ground.

Both the cases of an overall hard ground and that of a combined hard–soft ground were considered. In this latter case, the soft ground on the receiver's side was realized through setting an absorbing surface on the hard floor. Fig. 10 shows the frequency curves of the sound level without barrier, and where the effect of the impedance discontinuity is clearly manifested by the lower sound pressure level.

Finally, Fig. 11 illustrates the insertion loss curves for different angles of the wedge barrier.

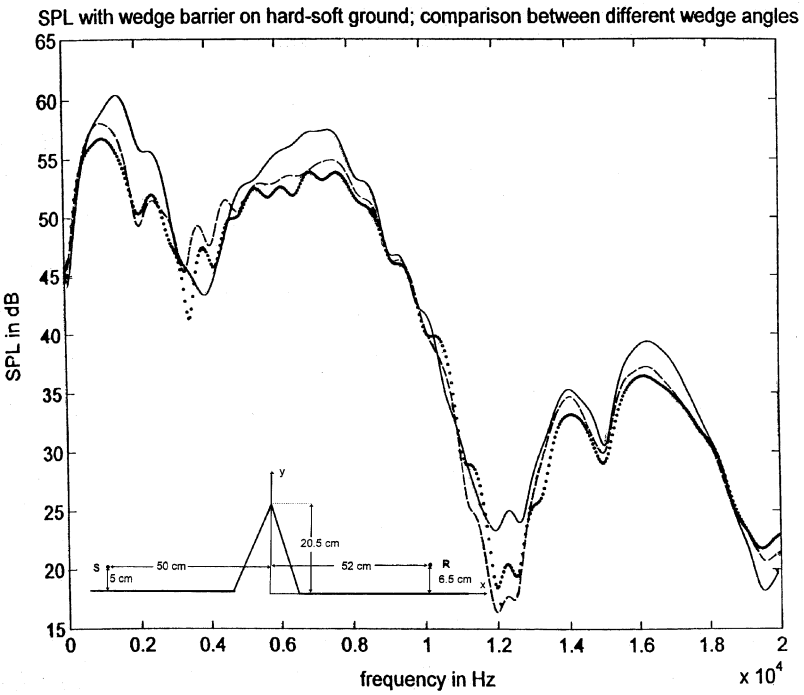


Fig. 11. Sound pressure level curves for a hard wedged barrier on hard–soft ground. ● ● ● ● ● ● ●: $w = 0°$, ------: $w = 30°$, ———: $w = 90°$.

The overall worsening of the IL of the wedge barrier is clearly seen for an increasing wedge angle, the decrease amounting to approximately 1 dB per 15° increase of the wedge angle. The case of a completely hard ground on both sides of the barrier is also found to be detrimental as compared to a partly absorbing ground.

## 6. Conclusions

This study was concerned with the problem of sound attenuation by a hard wedge-like barrier. The two approximate models, the UTD and the H–P model, used for treating the phenomenon of wave diffraction at the tip of the wedge show excellent agreement with the exact B–T theory. However, as the B–T theory and the H–P model require quite advanced mathematical and computational implementations, the UTD is then proposed as an efficient calculation scheme for considering most engineering applications of the type considered in the present study.

From this study, it has been possible to confirm from theoretical considerations that the amplitude of the edge-diffracted wave increases for an increasing angle of the wedge. For problems with typical distances of the same order of the size of a wavelength, the increase of the amplitude is monotonous and in the order of 0.5 dB per 10° increase of the wedge angle. These observations are also valid for a hard wedge-shaped barrier on the ground. In conclusion, for barriers with the same height, the classical thin barrier, with a suitable surface weight is the most efficient means for the reduction of noise.

## Acknowledgements

This work is part of a project supported by a grant from TeknikBroStiftelsen in Lund, and this is gratefully acknowledged.

## References

[1] J.J. Bowman, T.B.A. Senior, P.L.E. Uslenghi, Electromagnetic and Acoustic Scattering by Simple Shapes, 2nd Edition, Hemisphere, New York, 1987.
[2] H.M. Macdonald, A class of diffraction problems, Proceedings of the London Mathematical Society 14 (1915) 410–427.
[3] T.J. Bromwich, Diffraction of waves by a wedge, Proceedings of the London Mathematical Society 14 (1915) 450–463.
[4] F.J.W. Whipple, Diffraction by a wedge and kindred problems, Proceedings of the London Mathematical Society 16 (1919) 481–500.
[5] H.S. Carslaw, Diffraction of waves by a wedge of any angle, Proceedings of the London Mathematical Society 19 (1920) 291–306.
[6] F. Oberhettinger, Diffraction of waves by a wedge, Communications on Pure and Applied Mathematics 7 (1954) 551–563.
[7] F. Oberhettinger, On the diffraction and reflection of waves and pulses by wedges and corners, The Journal of Research of the National Bureau of Standards 61 (1958) 343–365.
[8] M.G. Garnir, Fonctions de Green de l'opérateur metaharmonique pour les problèmes de Dirichlet et de Neumann posés dans un angle ou un Dièdre, Bulletin de la Société Royale de Liège 21 (1952) 207–231.
[9] F.G. Friedlander, Sound Pulses, Cambridge University Press, New York, 1958.
[10] G.D. Maliuzhinets, Excitation, reflection and emission of surface waves from a wedge with given face impedances, Soviet Physics Doklady 3 (1958) 752–755.
[11] V.K. Kusnetzov, A new method for solving the problem of the sound field in a fluid wedge, Soviet Physics Acoustics 51 (1959) 171–176.
[12] A.V. Osipov, A.N. Norris, The Maliuzhinets theory for scattering from wedge boundaries: a review, Wave Motion 29 (1999) 313–340.
[13] A.A. Thuzilin, New representation of diffraction fields in wedge-shaped regions with ideal boundaries, Soviet Physics Acoustics 9 (1963) 168–172.
[14] M.A. Biot, I. Tolstoy, Formulation of wave propagation in infinite media by normal coordinates with an application to diffraction, Journal of the Acoustical Society of America 29 (1957) 381–391.
[15] I. Tolstoy, Exact explicit solutions for diffraction by hard sound barriers and sea mounts, Journal of the Acoustical Society of America 85 (1989) 661–669.
[16] I. Tolstoy, Diffraction by a hard truncated wedge and a strip, IEEE Transactions on Ocean Engineering 14 (1989) 4–16.
[17] M.J. Buckingham, I. Tolstoy, An analytical solution for benchmark problem I: the 'ideal' wedge, Journal of the Acoustical Society of America 87 (1990) 1511–1513.
[18] J.B. Keller, A. Blank, Diffraction and reflections of pulses by wedges and corners, Communications on Pure and Applied Mathematics 4 (1951) 75–94.
[19] S.W. Lee, Y. Rahmat-Samii, R.C. Menendez, GTD, ray field, and comments on two papers, IEEE Transactions on Antennas and Propagation AP-32 (1978) 352–356.
[20] O.M. Büyüdkura, GTD solution with higher order terms to the diffraction by an edge: towards a uniform solution, IEEE Proceedings on Microwaves, Antennas and Propagation 143 (1996) 43–50.
[21] T. Kawai, Sound diffraction by a many sided barrier or pillar, Journal of Sound and Vibration 79 (1981) 229–242.
[22] A.Z. Elsherbeni, M. Hamid, Diffraction by a wide double wedge, IEEE Transactions on Antennas and Propagation AP-32 (1984) 1262–1265.

[23] J.S. Robertson, Sound propagation over a large wedge: a comparison between the geometrical theory of diffraction and the parabolic equation, Journal of the Acoustical Society of America 106 (1999) 113–119.
[24] R.G. Kouyoumjian, P.H. Pathak, A uniform asymptotic theory of diffraction for an edge in a perfectly conducting surface, Proceedings of the IEEE 62 (1974) 1448–1461.
[25] P. Ambaud, A. Bergassoli, Le problème du Dièdre en acoustique, Acustica 27 (1972) 291–298.
[26] A.D. Pierce, Diffraction of sound around corners and over wide barriers, Journal of the Acoustical Society of America 55 (1974) 941–955.
[27] W.T. Hadden, A.D. Pierce, Sound diffraction around screens and wedges for arbitrary point source locations, Journal of the Acoustical Society of America 69 (1981) 1266–1276.
[28] W.T. Hadden, A.D. Pierce, Diffraction of sound around corners and over wide barriers (Erratum), Journal of the Acoustical Society of America 71 (1982) 1290.
[29] F.P. Mechel, Scattering at rigid building corners, Journal of Sound and Vibration 219 (1999) 105–132.
[30] W.E. Williams, Diffraction of an E-polarized plane wave by an imperfectly conducting wedge, Proceedings of the Royal Society of London A 252 (1959) 376–393.
[31] G.L. James, Uniform diffraction coefficients for an impedance wedge, Electronic Letters 13 (1977) 403–404.
[32] A.D. Rawlins, Diffraction by a dielectric wedge, Journal of the Institute of Mathematical Applications 19 (1977) 231–279.
[33] R. Tiberio, G. Pelosi, G. Manara, A uniform GTD formulation for the diffraction by a wedge with impedance faces, IEEE Transactions on Antennas and Propagation AP-33 (1985) 867–872.
[34] T.B.A. Senior, Solution of a class of imperfect wedge problems for skew incidence, Radio Science 21 (1986) 185–191.
[35] R.G. Rojas, Electromagnetic diffraction by a wedge with impedance faces, IEEE Transactions on Antennas and Propagation AP-36 (1988) 956–970.
[36] T. Griesser, C.A. Balanis, Reflections, diffractions, and surface waves for an interior impedance wedge of arbitrary angle, IEEE Transactions on Antennas and Propagation AP-37 (1989) 927–935.
[37] G. Pelosi, S. Maci, R. Tiberio, A. Michaeli, Incremental length diffraction coefficients for an impedance wedge, IEEE Transactions on Antennas and Propagation AP-40 (1992) 1201–1210.
[38] G. Manara, R. Tiberio, G. Pelosi, P.H. Pathak, High frequency scattering from a wedge with impedance faces illuminated by a line source, Part I: diffraction, IEEE Transactions on Antennas and Propagation AP-41 (1993) 212–218.
[39] G. Manara, R. Tiberio, G. Pelosi, P.H. Pathak, High frequency scattering from a wedge with impedance faces illuminated by a line source, Part II: surface waves, IEEE Transactions on Antennas and Propagation AP-41 (1993) 877–883.
[40] G. Pelosi, G. Manara, P. Nepa, Diffraction by a wedge with variable-impedance faces, IEEE Transactions on Antennas and Propagation AP-44 (1996) 1335–1340.
[41] R.G. Kouyoumjian, G. Manara, P. Nepa, B.J.E. Taute, The diffraction of an inhomogeneous plane wave by a wedge, Radio Science 31 (1996) 1387–1398.
[42] H.H. Syed, J.L. Volakis, High frequency EM scattering by edges in artificially hard and soft surfaces illuminated at oblique incidence, IEEE Transactions on Antennas and Propagation 48 (1996) 790–800.
[43] G. Manara, P. Nepa, G. Pelosi, EM scattering from anisotropic impedance wedges illuminated at oblique incidence. The case of artificially hard and soft boundary conditions, Electromagnetism 18 (1998) 117–133.
[44] G. Pelosi, G. Manara, P. Nepa, Electromagnetic scattering by a wedge with anisotropic impedance faces, IEEE Transactions on Antennas and Propagation AP-46 (1998) 29–35.
[45] J.F. Rouviere, N. Douchin, P.F. Combes, Diffraction by lossy dielectric wedges using both heuristic UTD formulations and FDTD, IEEE Transactions on Antennas and Propagation AP-47 (1999) 1702–1708.
[46] G. Manara, P. Nepa, G. Pelosi, High frequency EM scattering by edges in artificially hard and soft surfaces illuminated at oblique incidence, IEEE Transactions on Antennas and Propagation AP-48 (2000) 790–800.
[47] H.G. Jonasson, Diffraction by wedges of finite acoustic impedance with applications to depressed roads, Journal of Sound and Vibration 25 (1972) 577–585.
[48] A.D. Pierce, W.J. Hadden, Plane wave diffraction by a wedge with finite impedance, Journal of the Acoustical Society of America 63 (1978) 17–27.

[49] D. Chu, Impulse response of density contrast using normal coordinates, Journal of the Acoustical Society of America 86 (1989) 1883–1896.
[50] A.M.J. Davis, Two-dimensional acoustical diffraction by a penetrable wedge, Journal of the Acoustical Society of America 100 (1996) 1316–1324.
[51] H. Syed, J.L. Volakis, An approximate solution for scattering by an impedance wedge at skew incidence, Radio Science 30 (1995) 505–524.
[52] H. Syed, J.L. Volakis, PTD analysis of impedance structures, IEEE Transactions on Antennas and Propagation AP-44 (1996) 983–988.
[53] P.M. Johansen, Uniform physical theory of diffraction equivalent edge currents for truncated wedge strips, IEEE Transactions on Antennas and Propagation AP-44 (1996) 989–995.
[54] D.I. Butorin, P.Y. Ufimtsev, Explicit expression for an acoustic edge wave scattered by an infinitesimal edge element, Soviet Physics Acoustics 32 (1987) 283–287.
[55] H.S. Hasnain, J.L. Volakis, PTD analysis of impedance structures, IEEE Transactions on Antennas and Propagation AP-44 (1996) 983–988.
[56] R.J. Luebbers, A heuristic UTD slope diffraction coefficient for rough lossy wedges, IEEE Transactions on Antennas and Propagation AP-37 (1984) 206–211.
[57] G. Stratis, V. Anantha, A. Taflove, Numerical calculation of diffraction coefficients of generic conducting and dielectric wedges using FDTD, IEEE Transactions on Antennas and Propagation AP-45 (1997) 1525–1529.
[58] N.Y. Zhu, F.M. Landstorfer, Numerical determination of diffraction, slope-, and multiple diffraction coefficients of impedance wedges by the method of parabolic equation: space waves, EEE Transactions on Antennas and Propagation AP-43 (1995) 1429–1435.
[59] F.P. Mechel, Modes in lined wedge-shaped ducts, Journal of Sound and Vibration 216 (1998) 649–671.
[60] F.P. Mechel, Modal analysis in lined wedge-shaped ducts, Journal of Sound and Vibration 216 (1998) 673–696.
[61] M.J. Buckingham, Theory of three-dimensional acoustic propagation in a wedge-like ocean with penetrable bottom, Journal of the Acoustical Society of America 82 (1987) 198–210.
[62] R.D. Graves, A. Nagl, H. Überall, G.L. Zarur, Range dependent normal modes in underwater sound propagation: application to the wedge-shaped ocean, Journal of the Acoustical Society of America 58 (1975) 1171–1177.
[63] L.B. Felsen, W.A. Kuperman, Sound propagation in a wedge shaped ocean with a penetrable bottom, Journal of the Acoustical Society of America 67 (1980) 1564–1566.
[64] J.M. Arnold, L.B. Felsen, Rays and local modes in a wedge-shaped ocean, Journal of the Acoustical Society of America 73 (1983) 1105–1119.
[65] W.A. Kinney, C.S. Clay, G.A. Saunders, Scattering from a corrugated surface: comparison between experiment Helmholtz–Kirchhoff theory and the facet-ensemble method, Journal of the Acoustical Society of America 73 (1983) 183–194.
[66] H. Medwin, Shadowing by finite noise barriers, Journal of the Acoustical Society of America 69 (1981) 1060–1064.
[67] A.I. Papadopoulos, C.G. Don, A study of barrier attenuation by using acoustic impulses, Journal of the Acoustical Society of America 90 (1991) 1011–1018.
[68] S.I. Thomasson, Reflection of waves from a point source by an impedance boundary, Journal of the Acoustical Society of America 59 (1976) 780–785.
[69] B.A. DeJong, A. Moerkerken, J.D. Van Der Toorn, Propagation of sound over grassland and over an earth Barrier, Journal of Sound and Vibration 86 (1983) 23–46.
[70] C.F. Chien, W.W. Soroka, A note on the calculation of sound propagation along an impedance surface, Journal of Sound and Vibration 69 (1980) 340–343.
[71] H. Medwin, E. Childs, G.M. Jebsen, Impulse studies of double diffraction: a discrete huygens interpretation, Journal of the Acoustical Society of America 72 (1982) 1005–1013.
[72] M.E. Delany, E.N. Bazley, Acoustical properties of fibrous absorbent materials, Applied Acoustics 3 (1970) 105–116.
[73] T.F.W. Embleton, J.E. Piercy, G.A. Daigle, Effective resistivity of ground surfaces determined by acoustical measurements, Journal of the Acoustical Society of America 74 (1983) 1239–1244.